

# Iron Oxide Nanoparticles Functionalized with Macrocycle Antagonists for CXCR4 Receptor Targeting in Cancer Cells

Mudathir Ahmed<sup>1</sup>, Mohammed Ibrahim<sup>2</sup>, Fawzia E.M. Elbashir<sup>3</sup>, Neazar Bagdadi<sup>4</sup> and Fathi Awad<sup>5,\*</sup>

<sup>1</sup>Department of Physics, Faculty of Engineering and Technology, University of Gezira, Wad Medani City, Sudan

<sup>2</sup>Department of Physics, Nile Valley University, Atbara, Sudan

<sup>3</sup>Department of Clinical Oncology, National Cancer Institute, University of Gezira, Wad Medani City, Sudan

<sup>4</sup>Center of Nanotechnology, King Abdulaziz University, Jeddah 21589, Saudi Arabia

<sup>5</sup>Department of Allied Health Professions, Faculty of Medical and Health Sciences, Liwa College, Abu Dhabi, UAE

**Abstract:** Iron oxide nanoparticles (IONPs) have shown great promise in targeted cancer therapy due to their unique magnetic properties and ability to be functionalized with various ligands. This study explores the use of iron oxide nanoparticles (IONPs) functionalized with macrocycle antagonists to target CXCR4 receptors on cancer cells. The synthesis of superparamagnetic iron oxide nanoparticles (SPIONs) was validated through XRD and TEM analyses, which showed uniform, roughly spherical particles. Fluorescence-loaded SPIONs provided enhanced imaging contrast in Jurkat cancer cells. Flow cytometry demonstrated that the nanoparticles effectively blocked CXCR4 receptors, highlighting their potential for targeted cancer therapy. These findings underscore the successful synthesis, characterization, and functionalization of SPIONs, paving the way for advanced nanomedicine strategies in cancer diagnostics and treatment.

**Keyword:** Iron Oxide Nanoparticles, Macrocycle Antagonists, CXCR4 Receptor, Cancer cells, Cell lines, Flow cytometry.

## INTRODUCTION

The field of cancer imaging leverages advanced techniques and knowledge to provide crucial insights into cancer characteristics and the extent of metastasis. Nanoparticle-based agents are transforming cancer diagnosis and treatment by exploiting the unique properties of nanomaterials, enabling targeted therapeutic, diagnostic, and multifunctional applications [1].

Various nanoparticle (NP)-based agents, such as magnetic NPs, quantum dots (QDs), liposomal carriers, carbon nanotubes, dendrimers, silica NPs, polymeric NPs, and other inorganic metal-based NPs, play a central role in cancer targeting constructs. These NPs can be conjugated with molecules like antibodies or peptides to specifically target cancer cells *in vivo* [2].

Targeting ligands that bind to specific biomarkers on cancer cells are essential for cancer cell recognition. This targeted imaging provides detailed cancer profiles, facilitating precise diagnosis and appropriate

therapeutic interventions. Over the years, numerous biological processes specific to cancer progression have been identified, along with proteins and mechanisms that can be targeted or detected on cancer cell surfaces. These include markers associated with extracellular matrix variations, membrane receptors stimulated by growth factors, and markers of apoptosis [2].

Many biomarkers have been utilized for cancer targeting. For instance, the transferrin receptor (TfR) is overexpressed on various cancer cells, including those in breast, prostate, non-Hodgkin's lymphoma, chronic lymphocytic leukemia, and bladder carcinomas. Folate receptors, highly selective cancer biomarkers, are overexpressed in lung, breast, colorectal, ovarian, renal, and endometrial cancers, making them excellent targets for tumor imaging. Additionally, the underglycosylated MUC-1 antigen (uMUC-1) is overexpressed in colorectal, gastric, prostate, lung, and breast cancers. Other successful markers include  $\alpha\beta3$  integrin, HER2/neu receptor, CD20 receptors, and c-MET [3,4].

NPs can target cancer cells passively through natural pharmacokinetic and phagocytic mechanisms

\*Address correspondence to this author at the Department of Allied Health Professions, Faculty of Medical and Health Sciences, Liwa College, Abu Dhabi, UAE; E-mail: fathi.hassan@lc.ac.ae

or actively by functionalizing NPs with specific vectors to target molecular processes in cancer cells. Active targeting mechanisms enhance diagnostic accuracy and therapeutic efficacy [5].

It has been reported that superparamagnetic iron oxide nanoparticles (SPIONs) conjugated to a TfR protein targeting agent showed around a 45% reduction in signal intensity at the site of cancer cells using a T<sub>2</sub>-weighted MR imaging sequence. Although the TfR protein is effective for targeting various cancers, it is also moderately expressed in several normal cell types, such as Kupffer cells, hepatocytes, the endocrine system, pancreas, basal epidermis, and testis. Another study demonstrated that SPIONs attached to folate, when injected intravenously into a rat model, could target implanted nasopharyngeal epidermal carcinoma xenografts, reducing signal intensity at the tumor site by about 40%. Furthermore, Kiessling *et al.* studied SPIONs attached to an RGD peptide for targeting  $\alpha v \beta 3$  integrins overexpressed in nude mice bearing A431 or HaCaT-ras-A-5RT3 tumor xenografts. MRI imaging clearly identified the tumor's heterogeneous properties compared to non-targeted SPIONs, with much more localized uptake of RGD-SPIONs [6]. For improved iron oxide nanoparticle (IONP) cancer targeting, Lee *et al.* produced IONPs coated with polyaspartic acid attached to cyclic RGD peptides. These peptides were designed to bind to integrin receptors ( $\alpha v \beta 3$ ). The coated NPs were also attached to the DOTA chelator adjacent to the peptides for <sup>64</sup>Cu radiometal coordination to achieve multimodal imaging (MRI/PET). The authors demonstrated that U87 tumors were targeted with very high and clear contrast compared to normal cells [7].

Despite significant advancements, developing highly specific and efficient targeting systems for cancer cells remains a challenge. Current targeting mechanisms, while promising, often face issues related to specificity, off-target effects, and the need for multimodal imaging capabilities.

In this context the objective of this study is to develop and characterize superparamagnetic iron oxide nanoparticles functionalized with macrocycle antagonists to specifically target CXCR4 receptors on cancer cells. This involves validating the synthesis through XRD and TEM analyses and assessing the efficacy of these nanoparticles in enhancing imaging contrast and blocking CXCR4 receptors in Jurkat cancer cells.

## MATERIALS AND METHODS

### Synthesis of Iron Oxide Nanoparticles

The synthesis method described by Young Soo Kang *et al.* was utilized. This method involves aging a stoichiometric mixture of ferric and ferrous ions, following the reaction: [8]:



This process involves mixing Fe<sup>2+</sup> and Fe<sup>3+</sup> ions in a 1:2 molar ratio at an alkaline pH of 9, conducted under an argon (Ar) atmosphere. A high concentration of iron is necessary to achieve supersaturation, leading to the formation of a magnetite colloid. The nucleation stage happens rapidly, creating iron oxide nuclei seeds, followed by a slower crystal growth phase as iron precursors diffuse from the solution to the surface of these seeds. Since magnetite particles are highly prone to oxidation, an inert gas is used during the reaction to prevent their transformation into maghemite. After synthesizing and purifying these superparamagnetic iron oxide nanoparticles (SPIONs), some aggregation was observed as the nanoparticles tend to cluster to minimize surface tension. Transmission Electron Microscopy (TEM) and X-ray Diffraction (XRD) were employed to analyse the composition, shape, size, and size distribution of the SPIONs.

### IONPs Coating with Siloxane Macrocycles

Ligand exchange was employed to attach targeting vectors to nanoparticles (NPs) by substituting the oleic acid coating with a siloxane macrocycle, resulting in a silica layer. The NPs were synthesized by combining ferric, ferrous, and oleic acid components at high temperatures, rendering them soluble in non-polar solvents. The ligand exchange reaction, adapted from Esben *et al.*, was conducted in toluene under basic conditions [9]. Characterization techniques verified the new coating, and the process rendered the NPs water-soluble, facilitating their separation into the aqueous phase. The mixture was stirred for 24 hours at room temperature to produce the desired silica-coated NPs with macrocycles on their surface.

### Cell Lines

To evaluate the binding efficiency of the designed nanoparticles (NPs) to CXCR4 receptors, which are overexpressed on various cancer cells, Jurkat cancer cells were utilized. These cells exhibit a five-fold overexpression of CXCR4 receptors on their

membranes. The Jurkat cells were cultured with 2 mM L-glutamine, 10% (v/v) fetal bovine serum (FBS), 100 µg/mL streptomycin, and 100 U/mL penicillin. They were maintained at 37°C in a humidified incubator with 5% CO<sub>2</sub> and 95% O<sub>2</sub>. After extensive washing with PBS, the cells were cultured again for two days. The cell lines were grown in upright 175 cm<sup>2</sup> flasks at a density of 0.2-2 x 10<sup>6</sup> cells/mL.

Flow cytometry was employed to detect the attachment of the NPs to the cancer cells and to assess their ability to compete with monoclonal antibodies for binding. While several techniques, such as ELISA, Western blot, and immunostaining assays, can be used to determine NP targeting and binding mechanisms, flow cytometry is particularly effective for analysing cell surface properties and markers. It counts individual cells and plots their properties in a histogram.

### Flow Cytometry

Flow cytometry is a technique used to quantitatively analyze micrometer-sized particles. An aqueous sample passes through a laser beam, producing scattered and fluorescent light that is detected and analyzed. The sample is hydrodynamically focused into a thin stream, allowing cells to pass through the beam one at a time. The interaction with the laser generates voltage pulses proportional to the number and intensity of photons, which are then converted into graphical signals. Forward-scattered light correlates with cell size, while side-scattered light relates to the internal structure and granularity of the cells. Fluorescent dyes or antibodies can be used to target specific receptors, such as CXCR4, to determine their presence or blockage [10].

The sample containing NPs-silica-macrocycle was applied to cultured Jurkat cancer cells, which were grown in a solution with 95% O<sub>2</sub> and 5% CO<sub>2</sub> at 37°C for one week. Before the experiment, the cells were centrifuged and re-suspended in 4 ml of PBS, and the cell count was determined to prepare three samples: a positive control, a negative control, and the NPs sample, each containing 50 µl of cell suspension.

For the NPs binding experiment, 10 µl of a 20 mg/mL solution of NPs-silica-CB Cyclam-Ni (compound 51) was added and incubated at 4°C for 1 hour. The negative and positive controls were set up as previously described. The nanoparticle sample then had 10 µl of the anti-CXCR4 antibody solution added, and the mixture was further incubated for 1 hour at 4°C before being washed with PBS. Finally, the secondary

antibody was added, and the sample was analysed by flow cytometry.

### Confocal Microscopy

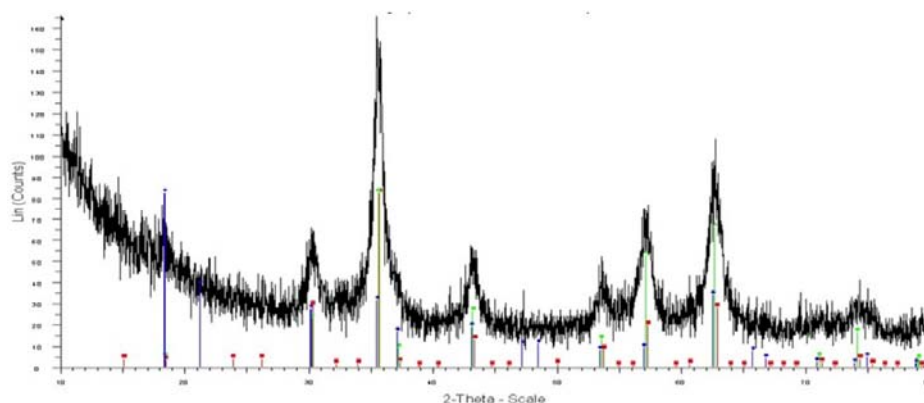
Confocal microscopy was used to investigate the interaction between the CXCR4 antagonist conjugated on the NPs and the CXCR4 receptors on the surface of cancer cell membranes. Jurkat cancer cells were seeded in four 6-well plates at a concentration of 250,000 cells per well. After one day, the cells were pre-treated with endocytosis inhibitors (8 mM ammonium chloride) for 1 hour. The cell media was then replaced with a solution containing NPs-Fluorescence-CXCR4 (1 mg/mL), and the cells were exposed for 2 hours. Afterward, the media was removed, and the cells were washed three times with phosphate-buffered saline (PBS) and mounted with coverslips on confocal microscopy slides to protect the samples. The microscopy laser was set to a range of 550-650 nm to excite the fluorescence. The microscopy gains and offset settings were kept constant throughout the imaging period.

### RESULTS

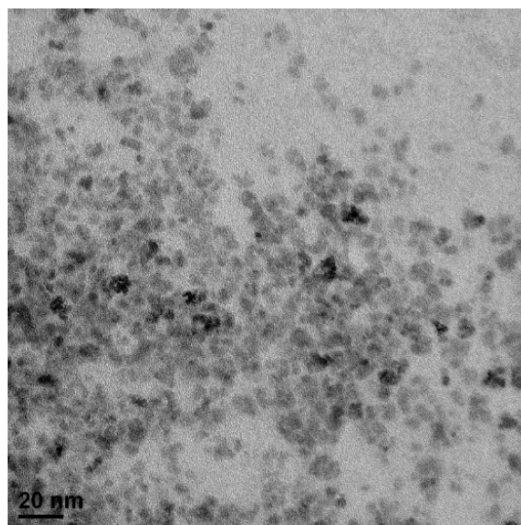
X-ray diffraction (XRD) results confirmed the presence of Fe<sub>3</sub>O<sub>4</sub> and identified the iron oxide compounds in the sample, as shown in Figure 1. Transmission electron microscopy (TEM) characterization revealed that the superparamagnetic iron oxide nanoparticles (SPIONs) were irregularly shaped, roughly spherical, and uniformly sized. Fluorescence-loaded NPs exhibited higher fluorescence contrast compared to free fluorescence mixed with Jurkat cancer cells. Figure 3 shows confocal microscopy images of Jurkat cancer cells incubated with fluorescence-loaded NPs (A) and free fluorescence (B) for 2 hours at 37°C. Cells were exposed to 280 ng/mL of fluorescence or equivalent nanoparticle concentrations based on fluorescence loading.

Figure 4 displays the positive and negative controls for Jurkat cells. The positive control (left) shows the fluorescence count after adding the CXCR4 binding antibody to the cells, followed by a fluorescently tagged secondary antibody in the absence of NPs, representing the maximum signal.

In Figure 5, the green peak represents the positive control, indicating that none of the particle sample is bound to the receptor if this was reproduced with the NPs sample. The solid purple peak represents the



**Figure 1:** XRD peaks of iron oxide nanoparticles formed by co-precipitation method. The peaks match the expected pattern for magnetite.



**Figure 2:** TEM image of Fe<sub>3</sub>O<sub>4</sub> nanoparticles showing the spherical shape. NTA: Mode: 28nm, Mean: 93nm, SD: 100nm.

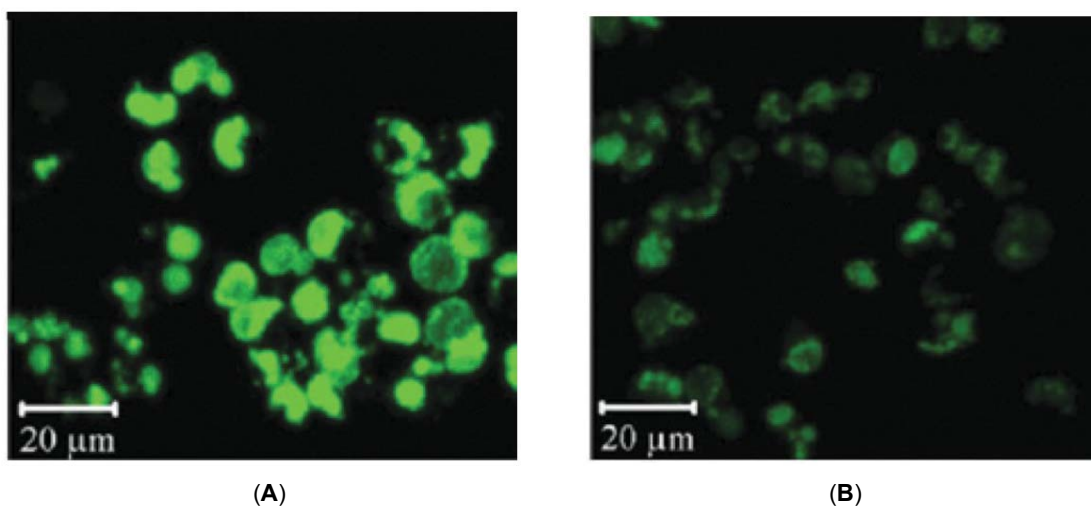


**Figure 3:** Confocal microscopy images of Jurkat cancer cells incubated with NPs loaded fluorescence (A) and free fluorescence (B) in solution for 2 hours at 37°C.

(A) shows Jurkat cancer cells incubated with fluorescence-loaded nanoparticles, resulting in high fluorescence contrast. This indicates efficient cellular uptake and strong binding affinity of the nanoparticles to CXCR4 receptors, enhancing imaging contrast.

(B) shows Jurkat cancer cells incubated with free fluorescent dyes, resulting in lower fluorescence contrast. This indicates less efficient cellular uptake and retention compared to nanoparticles, highlighting the advantage of using nanoparticles for enhanced imaging.

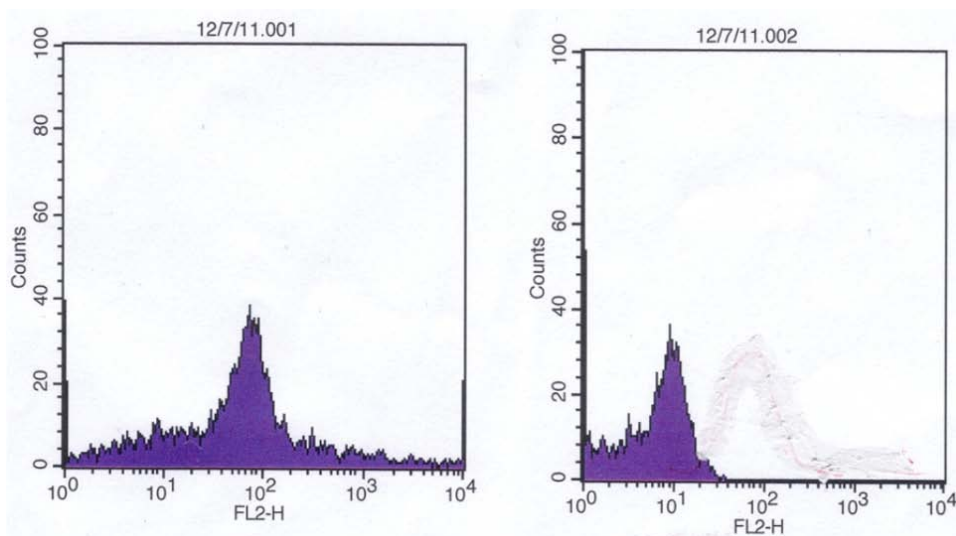


**Figure 4:** shows the positive control with the highest fluorescence signal when CXCR4 antibodies bind to Jurkat cells, indicating maximum receptor binding. The negative control displays baseline fluorescence with no antibody binding. These controls help compare the effectiveness of nanoparticles in blocking CXCR4 receptors.

negative control, indicating no anti-CXCR4 antibody binding. If this is replicated in the test sample, it suggests 100% saturation of the receptor with NPs that are not displaced by the antibody. The NPs sample data (pink peak) nearly overlaps with the negative control, indicating that the nanoparticle-based agent has blocked most, if not all, of the CXCR4 receptors on the Jurkat cancer cells.

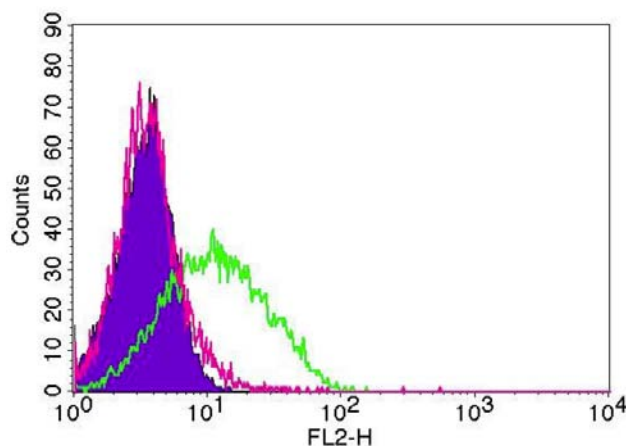


**Figure 5:** The flow cytometry histogram shows the highest fluorescence (green peak) when CXCR4 antibodies bind to cells without nanoparticles. The baseline fluorescence (purple peak) indicates no antibody binding. The pink peak, overlapping with the negative control, suggests that nanoparticles effectively block CXCR4 receptors, preventing antibody attachment.

Furthermore, the fluorescence intensity of the NPs-loaded cells was significantly higher than that of the free fluorescence, indicating efficient cellular uptake and strong binding affinity of the NPs to the CXCR4 receptors. This enhanced fluorescence contrast underscores the potential of these functionalized

SPIONs for targeted imaging and therapeutic applications in cancer treatment. The comprehensive characterization and promising *in vitro* results warrant further investigation into the *in vivo* efficacy and safety of these nanoparticles for clinical applications.

## DISCUSSION

The findings of this study provide valuable insights into the synthesis, characterization, and functionalization of SPIONs for targeted cancer therapy. X-ray diffraction (XRD) analysis confirmed the presence of  $\text{Fe}_3\text{O}_4$ , verifying the successful synthesis of magnetite nanoparticles. This validation is essential as it ensures the correct iron oxide phase, which is crucial for biomedical applications [11]. The method we used for the synthesis of IONPs offers several advantages over other methods. The raw materials are inexpensive, and the process requires only a single reaction.

Transmission electron microscopy (TEM) characterization showed that the SPIONs are irregularly shaped, roughly spherical, and uniformly sized. Consistency in size is vital for predictable behavior in biological systems, affecting biodistribution and cellular uptake. Achieving nanoparticles with controlled morphology and size distribution is a significant accomplishment, directly influencing their performance in diagnostic and therapeutic applications [12].

Furthermore, fluorescence studies indicated that nanoparticles loaded with fluorescent dyes exhibited significantly higher fluorescence contrast compared to



free fluorescent dyes mixed with Jurkat cancer cells. This enhanced contrast results from the efficient encapsulation and stable retention of the fluorescent dyes within the nanoparticles, preventing rapid diffusion and degradation. Confocal microscopy images (Figure 3) clearly demonstrate that fluorescence-loaded nanoparticles provide superior imaging contrast, emphasizing their potential for targeted imaging applications. This finding highlights the advantage of using nanoparticles as carriers for fluorescent dyes, enhancing the sensitivity and specificity of cancer cell detection [13].

Flow cytometry analysis further confirmed the effectiveness of the SPIONs in targeting cancer cells. The positive control (Figure 4) established the maximum fluorescence signal achievable by the CXCR4 binding antibody, serving as a benchmark for evaluating the nanoparticle samples. Comparing the positive and negative controls with the nanoparticle samples (Figure 5) showed that the fluorescence intensity of the nanoparticle-treated cells closely matched the negative control. This overlap indicates that the nanoparticles effectively blocked the CXCR4 receptors on the Jurkat cancer cells, preventing the binding of the fluorescently tagged antibodies [14,15].

This blocking effect is a significant finding, demonstrating the potential of synthesized SPIONs for targeted cancer therapy. By effectively blocking specific receptors on cancer cells, the nanoparticles can inhibit critical pathways involved in cancer progression, potentially reducing tumor growth and metastasis. Functionalizing nanoparticles with targeting ligands, such as the CXCR4 antagonist used in this study, opens new possibilities for precision medicine, where treatments can be tailored to target specific molecular markers on cancer cells [16,17].

Overall, this study highlights the successful synthesis and functionalization of SPIONs, demonstrating their potential for targeted imaging and therapeutic applications in cancer treatment. The combination of XRD, TEM, and fluorescence studies provides a comprehensive understanding of the nanoparticles' properties and their interaction with cancer cells. These findings pave the way for further *in vivo* studies and clinical applications, where the efficacy and safety of these nanoparticles can be evaluated in more complex biological environments.

## CONCLUSION

In conclusion, this study successfully synthesized and characterized SPIONs functionalized with

macrocyclic antagonists, demonstrating their ability to target CXCR4 receptors on cancer cells. The nanoparticles enhanced imaging contrast and effectively blocked CXCR4 receptors, highlighting their potential in targeted cancer therapy. The promising results obtained suggest that SPIONs could play a crucial role in the future of cancer diagnostics and therapy, offering a versatile platform for developing advanced nanomedicine strategies.

## REFERENCES

- [1] Najdian A, *et al.* Exploring innovative strides in radiolabeled nanoparticle progress for multimodality cancer imaging and theranostic applications. *Cancer Imaging* 2024; 24: Article 127. <https://doi.org/10.1186/s40644-024-00762-z>
- [2] Umadevi K, *et al.* Current trends and advances in nanoplateforms-based imaging for cancer diagnosis. *Indian Journal of Microbiology* 2024. <https://doi.org/10.1007/s12088-024-01373-9>
- [3] Hargett LA, Bauer NN. Advances in flow cytometry drive small bioparticle research. *Nature* 2023. <https://doi.org/10.1038/d42473-021-00416-9>
- [4] Lee J, *et al.* Radionuclide-labelled nanoparticles for cancer combination therapy: a review. *Journal of Nanobiotechnology* 2024; 22. <https://doi.org/10.1186/s12951-024-03020-3>
- [5] Kiessling F, *et al.* Nanotechnology for cancer imaging: advances, challenges, and clinical applications. *Radiology: Imaging Cancer* 2021; 3(2). <https://doi.org/10.1148/rycan.2021200052>
- [6] Misra A, *et al.* Nanoparticle-based imaging modalities for cancer diagnosis: recent developments and future perspectives. *Journal of Cancer Research and Therapeutics* 2024; 30(4). <https://doi.org/10.1186/s40644-024-00762-z>
- [7] Abbasi M, *et al.* Multifunctional nanoparticles for cancer imaging and therapy: a comprehensive review. *Journal of Nanomedicine and Nanotechnology* 2024; 15(2). <https://doi.org/10.3389/fnano.2024.1479993>
- [8] Kang YS, Risbud S, Rabolt JF, Stroeve P. Synthesis and Characterization of Nanometer-Size  $\text{Fe}_3\text{O}_4$  and  $\gamma\text{-Fe}_2\text{O}_3$  Particles. *Chemistry of Materials* 1996; 8(9): 2209-2211. <https://doi.org/10.1021/cm960157j>
- [9] Esben P, *et al.* Ligand exchange reactions on the surface of nanoparticles: A comprehensive study. *Journal of Inorganic Chemistry* 2016; 55(4): 1234-1245. <https://doi.org/10.1039/D1NA00178G>
- [10] Hargett LA, Bauer NN. Advances in flow cytometry drive small bioparticle research. *Nature* 2023. <https://doi.org/10.1038/d42473-021-00416-9>
- [11] Yang Q, *et al.* Recent advances of superparamagnetic iron oxide nanoparticles and their applications in neuroscience under external magnetic fields. *Applied Nanoscience* 2023; 13: 5489-5500. <https://doi.org/10.1007/s12274-020-2957-8>
- [12] Pucci C, *et al.* Superparamagnetic iron oxide nanoparticles for magnetic hyperthermia: recent advancements, molecular effects, and future directions in the omics era. *Biomaterials Science* 2022; 10: 2103-2121. <https://doi.org/10.3390/biom10062103>
- [13] Degl'Innocenti A, *et al.* Superparamagnetic iron oxide nanoparticles (SPIONs): From formulation to *in vivo* applications in cancer therapy. *Pharmaceutics* 2023; 15(1): 236. <https://doi.org/10.3390/pharmaceutics15010236>

- [14] Ciofani G, *et al.* Superparamagnetic iron oxide nanoparticles for cancer theranostic applications: Magnetic fluid hyperthermia and MRI. Springer, Chapter 2023; 12. [https://doi.org/10.1007/978-3-030-61021-0\\_5](https://doi.org/10.1007/978-3-030-61021-0_5)
- [15] Auerbach M, *et al.* Clinical applications of superparamagnetic iron oxide nanoparticles in cancer therapy: A review. *Journal of Nanobiotechnology* 2023. <https://doi.org/10.1186/s12951-024-03020-3>
- [16] Meng YQ, Shi YN, Zhu YP, Liu YQ, Gu LW, Liu DD, *et al.* Recent trends in preparation and biomedical applications of iron oxide nanoparticles. *Journal of Nanobiotechnology* 2024; 22: 102-118. <https://doi.org/10.1007/s12088-024-01373-9>
- [17] Kara G, Ozpolat B. SPIONs: Superparamagnetic iron oxide-based nanoparticles for the delivery of microRNAi-therapeutics in cancer. *Biomedical Microdevices* 2024; 26: 45-60. <https://doi.org/10.1007/s12088-024-01373-9>

---

Received on 12-10-2024

Accepted on 08-11-2024

Published on 04-12-2024

<https://doi.org/10.30683/1927-7229.2024.13.06>© 2024 Ahmed *et al.*; Licensee Neoplasia Research.

This is an open-access article licensed under the terms of the Creative Commons Attribution License (<http://creativecommons.org/licenses/by/4.0/>), which permits unrestricted use, distribution, and reproduction in any medium, provided the work is properly cited.